SUPPLEMENTARY INFORMATION

Compelling DNA Intercalation through "Anion-Anion" Anti-Coulombic Interaction: Boron Nanocarriers as Promising Anticancer Agents

Laura Gutiérrez-Gálvez,[1] Tania García-Mendiola,[1,2] Encarnación Lorenzo,[1,2,3] Miquel Nuez-Martinez,[4] Carmen Ocal,[4] Shunya Yan,[4] Francesc Teixidor,[4] Teresa Pinheiro[5,6], Fernanda Marques,[6,7] Clara Viñas.[4,*]

[1] Departamento de Química Analítica y Análisis Instrumental. Universidad Autónoma de Madrid. 28049, Madrid, Spain.

[2]Institute for Advanced Research in Chemical Sciences (IAdChem). Universidad Autónoma de Madrid. 28049, Madrid, Spain.

[3] IMDEA-Nanociencia, Ciudad Universitaria de Cantoblanco. 28049, Madrid (Spain).

[4] Institut de Ciència de Materials de Barcelona (C.S.I.C.) Campus U.A.B. 08193 Bellaterra, Barcelona. Spain.

[5] iBB - Instituto de Bioengenharia e Biociências, Instituto Superior Técnico, Universidade de Lisboa, Av. Rovisco Pais 1, 1049-001 Lisboa, Portugal.

[6] Departamento de Engenharia e Ciências Nucleares, Instituto Superior Técnico, Universidade de Lisboa, Estrada Nacional 10, 2695-066 Bobadela LRS, Portugal.

[7] C[2]TN - Centro de Ciências e Tecnologias Nucleares, Instituto Superior Técnico, Universidade de Lisboa, Estrada Nacional 10, 2695-066 Bobadela LRS, Portugal.

* Correspondence: clara@icmab.es

Figure S1. XPS spectra of the nanohybrid CT-*ds*DNA/Na[*o*-FESAN] (orange), Na[*o*-FESAN] (grey) and, CT-*ds*DNA (blue). The first top panel shows the survey spectra for the trhee cases and the rest of the panels are the short range spectra for the following core levels: a) C 1s, b) B 1s (a sub-peak at 186 eV appears in the nano-hybrid), c) Na 1s, d) N 1s, e) P 2p and f) Fe 2p ($2p_{1/2}$, $2p_{3/2}$).

Figure S2. Cyclic voltammograms of 3.0 mM *ds*DNA/Na[*o*-FESAN] (orange line) and Na[*o*-FESAN] (grey line) in 0.1 M PB pH 7.0 solution at a AuSPE. Scan rate is 100 mV/s.

Figure S3. a) Absorption spectra of Na[*o*-FESAN] at different concentrations. Inset: Plot of the absorbance *v*s concentration of Na[*o*-FESAN]. b) Absorption spectra of Na[*o*-FESAN] from the solution discarded in the centrifugation step (dilution 1:100). c) Absorption spectra of nanohybrid CT-*ds*DNA/Na[*o*-FESAN].

Figure S4. Left: Differential Pulse Voltammograms at a AuSPE: (a) anodic and (c) cathodic peak, respectively, of 2.0 mM CT-dsDNA (red line) and after addition of increasing concentrations of Na[*o*-FESAN] (colored lines) from 1.0 to 20.0 mM in 0.1 M PB pH 7.0 solution. Right: potential peaks (E) of the anodic (b) and cathodic (d) scan vs the Na[*o*-FESAN] concentration from plots (a) and (c), respectively.

Figure S5. Calibration plot of the absorbance (measured by AAS) *v*s Fe concentration in mM. Points presented are the media of three determinations.

Identification and local distribution of materials by Friction Force Microscopy. Concepts and details of the analysis methodology.

Figure S6. Topographic profiles (left) across different single layers exposed at the topmost surface of the [*o*-FESAN]$^-$ needle-like crystallite in (a). To highlight the topographic details and provide clearer identification of the diverse layers forming the fiber (needle), the corresponding error signal channel is depicted in (b).

Figure S7. Friction analysis of the hybrid CT-*ds*ADN/Na[*o*-FESAN] (1:100) sample. At the figure left and middle top (bottom) are shown the lateral force forward (backwards) images corresponding to the topographies of Figure 7 - images a and c in the manuscript. Right panels from top to bottom are the topography profile and corresponding friction (green) data extracted from the separated lateral force profiles depicted in the bottom panel. All line profiles were taken at the same surface location for direct correlation between morphological details and chemical nature of the different surface regions. The Na[*o*-FESAN] fibers have a friction 75% lower than the surrounding DNA aggregates.

The irregular rim on the round perimeter of the structures has the same frictional contrast as the small aggregates extended over the surrounding areas.

Figure S8. a) ESI-MS spectra of the CT-*ds*DNA/Na[*o*-FESAN] nanohybrid at the **positive mode**. b) ESI-MS spectra of the CT-*ds*DNA/Na[*o*-FESAN] nanohybrid at the **negative mode**; peak displays isotopic (-1) distribution. c) Magnification of the positive mode in the range 400-650 m/z; the peaks display isotopic (+1) distribution.

Figure S9. a) MALDI-TOF-MS run in the range 199.0 – 5013.0 m/z at the **negative mode** in the **absence of matrix**: CT-*ds*DNA (at the top), the hybrid CT-*ds*DNA/Na[*o*-FESAN] diluted 100 times in H_2O (at the middle) and the hybrid CT-*ds*DNA/Na[*o*-FESAN] diluted 100 times in acetone (at the bottom). b) Spectrum of the CT-*ds*DNA (reference) with the corresponding peaks number that are the ones used in Table S2 for the assignation of the nanohybrids peaks.

Figure S10. Magnification of the MALDI-TOF-MS spectra at the negative mode of CT-*ds*DNA (blue) and CT-*ds*DNA/Na[*o*-FESAN] (red) samples diluted 100 times in water (Figure S9a top and middle) in the different zones: a) from 200 m/z to 1400 m/z; b) from 1400 m/z to 2600 m/z and c) 2600 m/z to 5000 m/z.

Figure S11. MALDI-TOF-MS spectra of the CT-*ds*DNA/Na[*o*-FESAN] nanohybrid diluted 100 times **in water** (up in red) and CT-*ds*DNA/Na[*o*-FESAN] nanohybrid diluted 100 time **in acetone** (down in marooned): a) from 200 m/z to 1400 m/z, b) from 1400 m/z to 2600 m/z and c) 2600 m/z to 5000 m/z.

Figure S12. MALDI-TOF-MS at the **negative mode** of CT-*ds*DNA (the reference). Range: 0-3500 Da; DHB (**matrix**); 70 (attenuation 30%); laser 7000 shots. Magnification at high molecular peaks.

Figure S13. a) MALDI-TOF-MS spectrum at the **negative mode** of the CT-*ds*DNA/Na[*o*-FESAN] nanohybrid diluted 100 times **in water**. Range: 0-3500 Da; **DHB** (matrix); 70 (attenuation 30%); laser 7000 shots. b) Magnification and theoretical mass spectra of the peaks at 437.28, 473.44 and, 647.61 m/z; (z=1).

Table S1. Elemental analysis of the dry nanohybrid CT-*ds*DNA/Na[o-FESAN] and the dry CT-*ds*DNA.

Table S2. The anodic peaks of the MALDI-TOF-MS spectra of the CT-*ds*DNA (as the reference) and the nanohybrid CT-*ds*DNA/Na[*o*-FESAN].

Table S3. Analysis of the XPS spectra of deconvoluted B 1s, P 2p and N 1s for the CT-*ds*DNA/Na[*o*-FESAN] nanohybrid, Na[*o*-FESAN]$^-$ and *ds*DNA. The indicated core level binding energy (BE) for each element and material sample has been determined using as in-situ reference the C 1s at 284.8eV (survey spectra in Figure S1 in the Supporting Information). New peaks, clearly appearing in the nan-hybrid material respect to the pure initial compounds, are indicated (∗). For simplicity, instead of total peak area, the Intensity given is the calculated peak height in counts per second (CPS) extracted from the experimental fits before (after) subtracting the adequate baseline or background intensity.

Figure S14. a) ^{11}B-NMR spectra of Na[*o*-FESAN] in D_2O with the chemical shift numbers of the Boron vertices B(6), B(5,11), B(9,12), B(10), B(4,7) and B(8) from down to high field.[1] b) ^{1}H-NMR spectra of Na[*o*-FESAN] in D_2O.[1] c) The CV wave of Na[*o*-FESAN]. $E_{1/2}$ = -1.00V versus F_c^+/F_c.[2] d) Solubility study of Na[3,3'-Fe(1,2-$C_2B_9H_{11})_2$], Na[*o*-FESAN] in H_2O; Plot of absorbance *vs.* concentration.[2]

Figure S1. XPS spectra of the nanohybrid CT-*ds*DNA/Na[*o*-FESAN] (orange), Na[*o*-FESAN] (grey) and, CT-*ds*DNA (blue). The first top panel shows the survey spectra for the trhee cases and the rest of the panels are the short range spectra for the following core levels: a) C 1s, b) B 1s (a sub-peak at 186 eV appears in the nano-hybrid), c) Na 1s, d) N 1s, e) P 2p and f) Fe 2p ($2p_{1/2}$, $2p_{3/2}$).

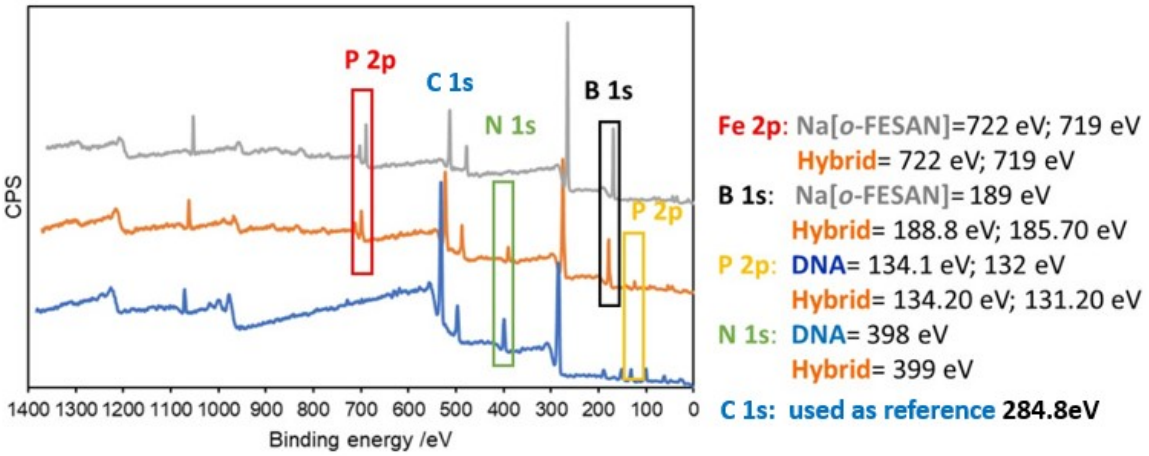

a) C 1s

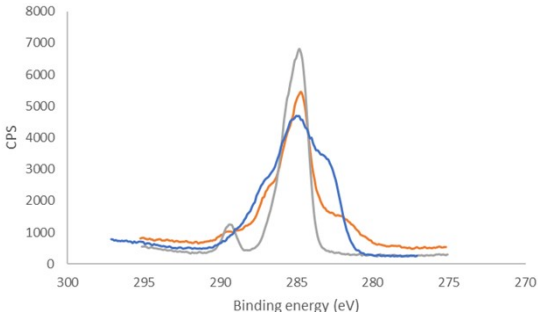

b) B 1s (a sub-peak at a 186 eV appears in the hybrid) lower BE of nano-

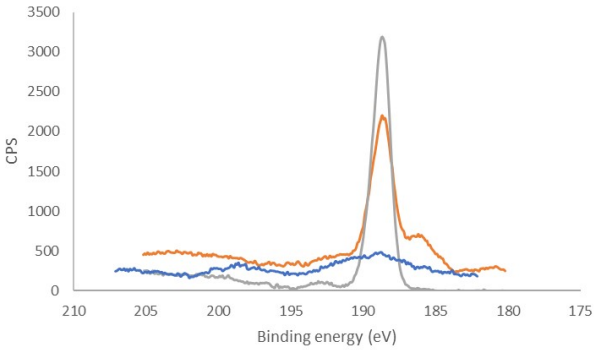

c) Na 1s

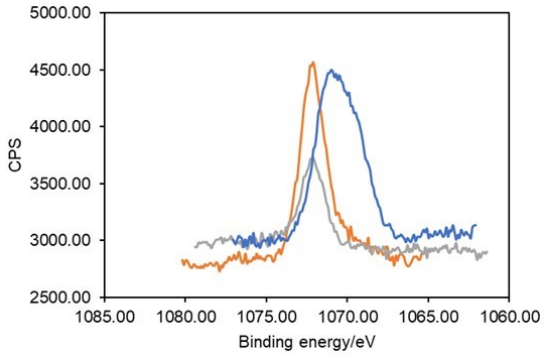

d) N 1s

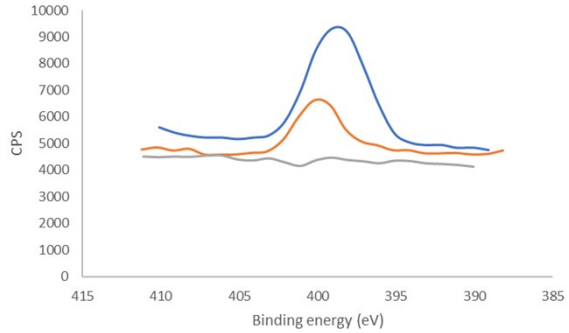

e) P 2p (showing a clear shift to higher BE)

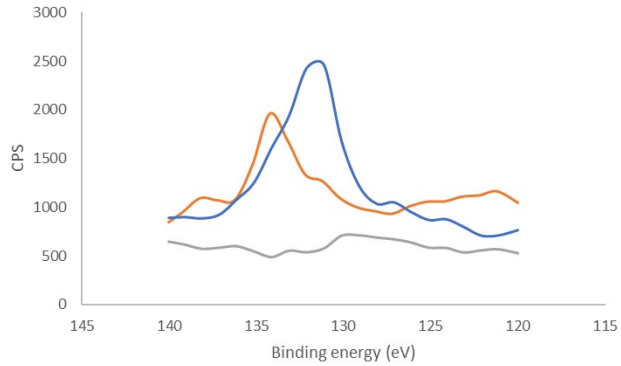

f) Fe 2p ($2p_{1/2}$, $2p_{3/2}$)

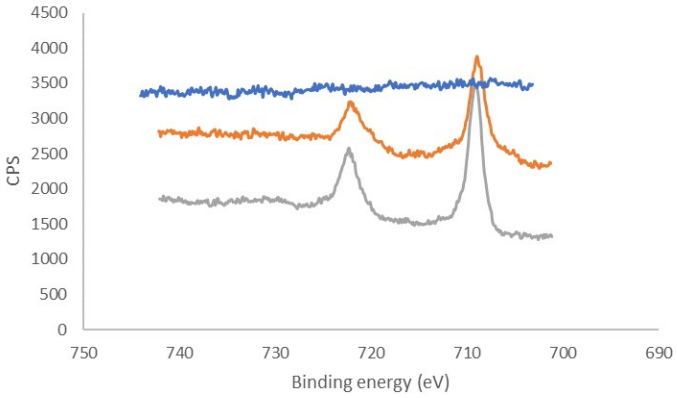

Figure S2. Cyclic voltammograms of 3.0 mM CT-*ds*DNA/Na[*o*-FESAN] (orange line) and Na[*o*-FESAN] (grey line) in 0.1 M PB pH 7.0 solution at a AuSPE. Scan rate is 100 mV/s.

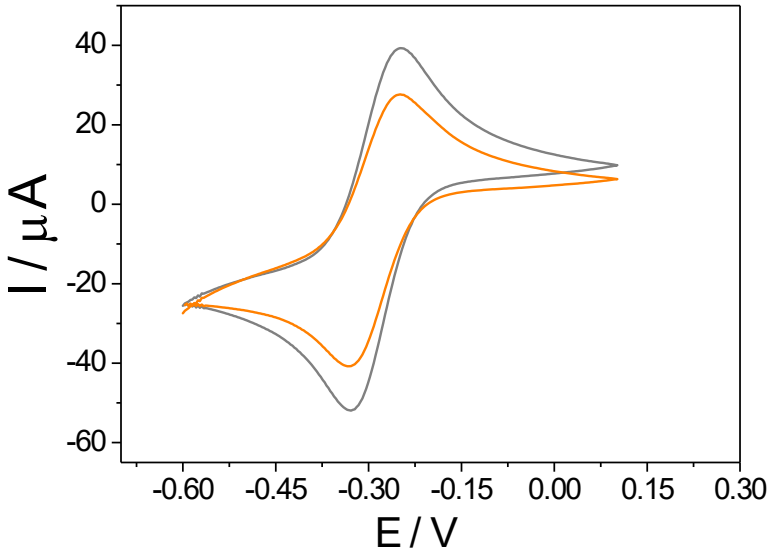

Figure S3. a) UV-visible absorption spectra of Na[*o*-FESAN] at different concentrations. Inset: Plot of the absorbance *vs* concentration of Na[*o*-FESAN]. b) Absorption spectra of Na[*o*-FESAN] from the solution discarded in the centrifugation step (dilution 1:100). c) Absorption spectra of nanohybrid CT-*ds*DNA/Na[*o*-FESAN].

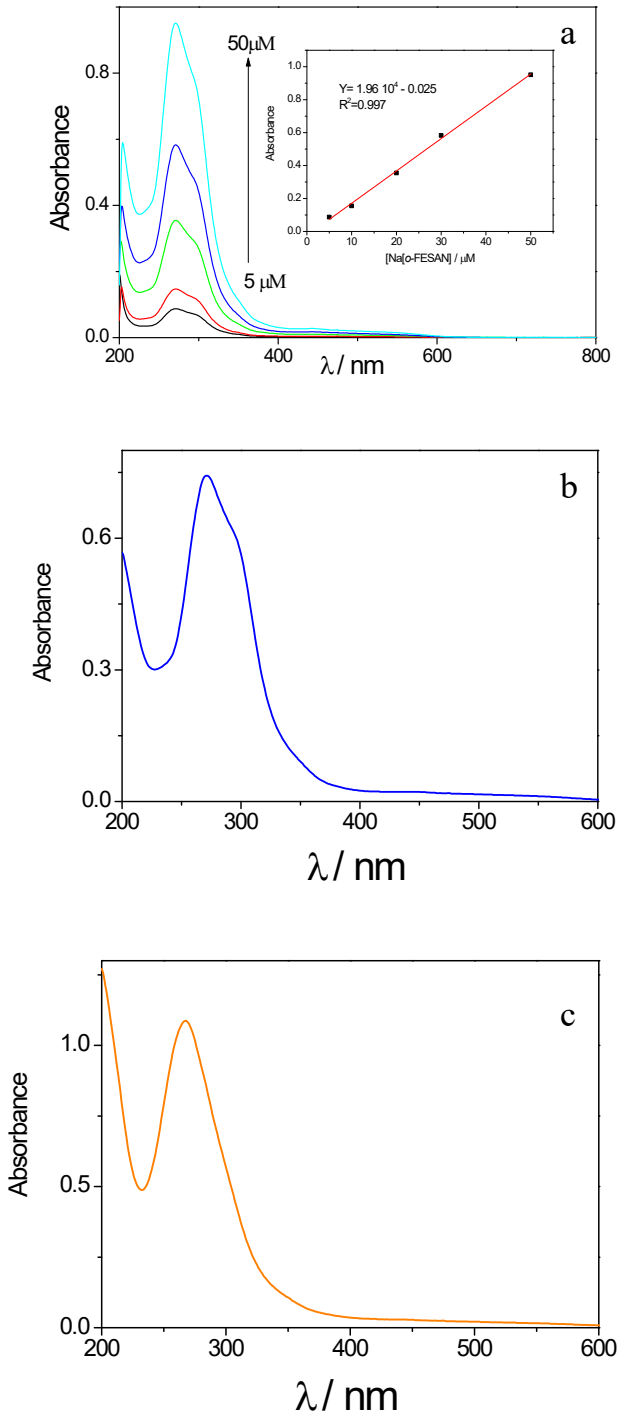

Figure S4. Left: Differential Pulse Voltammograms at a AuSPE: (a) anodic and (c) cathodic peak, respectively, of 2.0 mM CT-dsDNA (red line) and after addition of increasing concentrations of Na[*o*-FESAN] (colored lines) from 1.0 to 20.0 mM in 0.1 M PB pH 7.0 solution. Right: potential peaks (E) of the anodic (b) and cathodic (d) scan vs the Na[*o*-FESAN] concentration from plots (a) and (c), respectively.

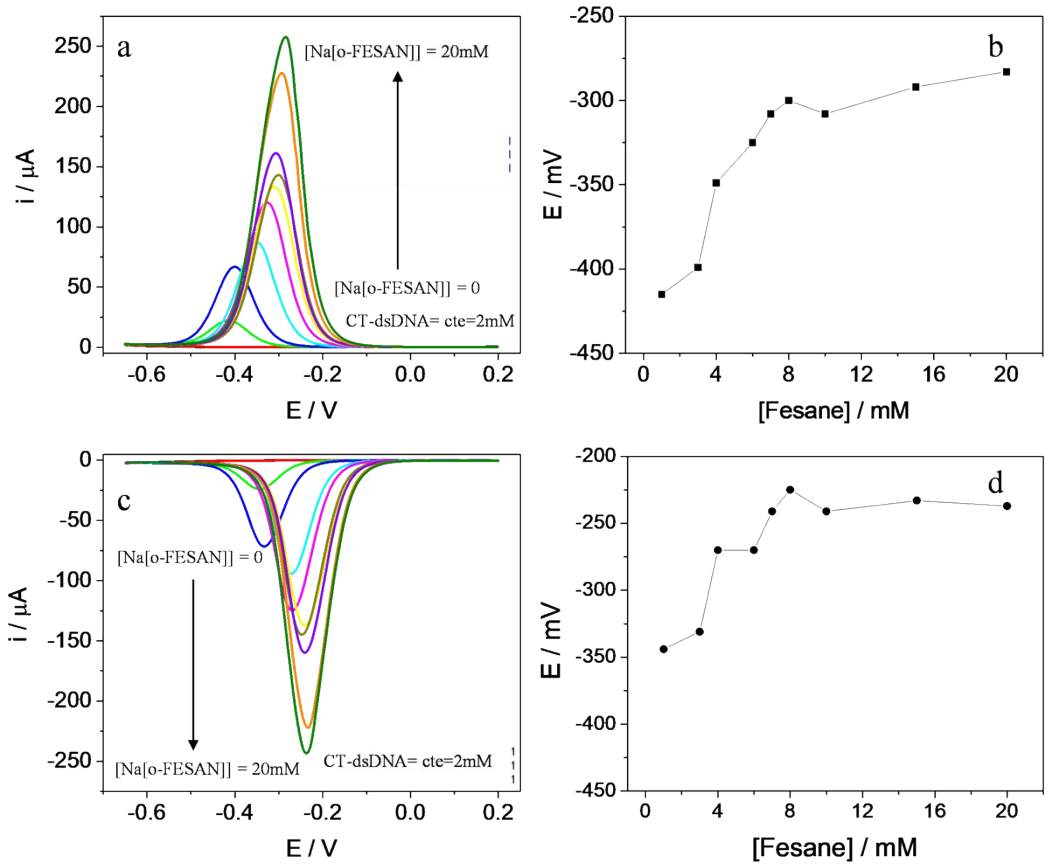

Figure S5. Calibration plot of the absorbance (measured by AAS) *vs* Fe concentration in mM. Points presented are the average of three determinations.

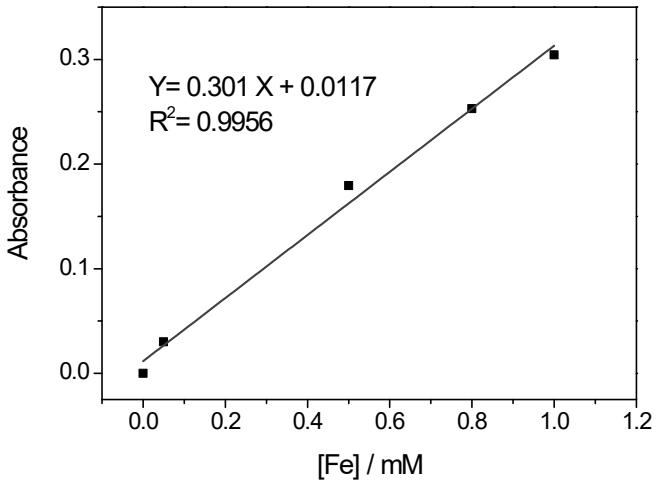

Identification and local distribution of materials by Friction Force Microscopy (FFM).

During tip scanning in AFM contact mode operation, in addition to cantilever normal deflection (topography), the cantilever torsion is monitored as a lateral deflection of the reflected laser beam. Since the lateral force caused by friction always opposes the tip motion, the tip twist reverses when the scan direction is inverted. Consequently, if a surface consists of regions with different friction, lateral force images will present opposite contrast in forward and backward directions. *Those regions of lower friction would appear as dark patches in the forward scans* and brighter in the backwards scans (Figure 2k – images d and f, Figure S14). The local friction signal is defined as half the amplitude of the so called friction loop, F = ½ [LF(f) – LF(b)], where FL(i) is the lateral force signal of the forward (i=f) and the corresponding backward (i=b) scans. This line by line procedure can be also applied to the complete lateral force images leading to FFM images or friction maps. Though forward (scanning from left to right) and backward (scanning from right to left) lateral force images are commonly recorded in contact AFM, in practice for qualitative analysis, only forward images are shown in which regions of lower(dark) and higher(light) friction are directly correlated to dark or light contrast, respectively. This technique is of particular interest for elucidating lateral inhomogeneity of a sample surface, because surface characteristics influencing the frictional properties can help visualizing regions of different nature (chemical composition, structural order…) such as graphene flakes in ceramic matrix, organic islands on metal substrates or to distinguish between two different chemical species in mixed self-assembled monolayers. Moreover, the investigation of the local frictional properties by means of FFM has shown to be a valuable tool to reveal structural details of molecular films which are difficult to visualize with other techniques.

Figure S6. Topographic profiles (left) across different single layers exposed at the topmost surface of the [*o*-FESAN]$^-$ needle-like crystallite in (a). To highlight the topographic details and provide clearer identification of the diverse layers forming the fiber (needle), the corresponding error signal channel is depicted in (b).

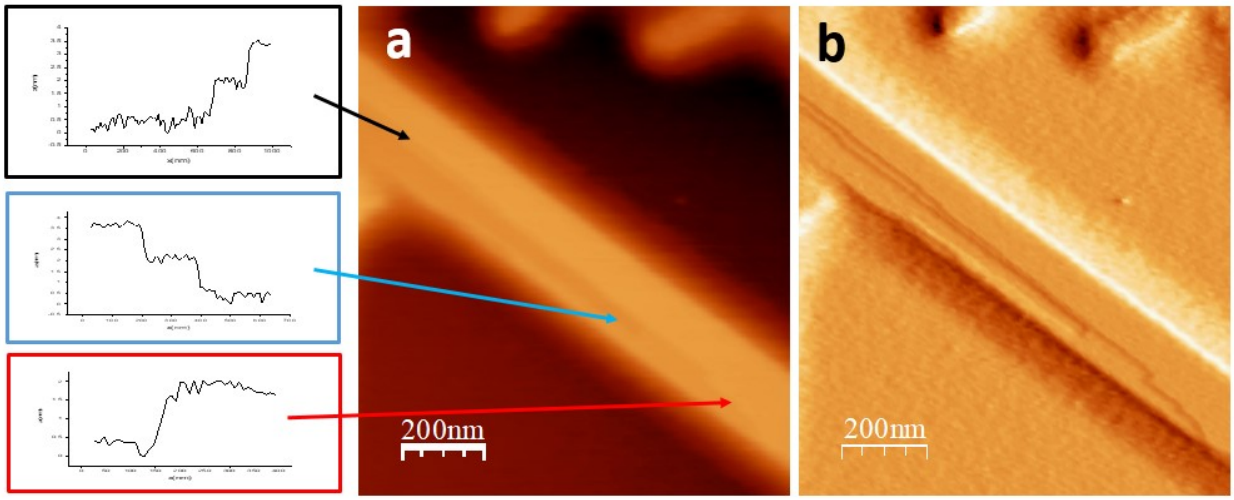

Figure S7. Friction analysis of the hybrid CT-*ds*ADN/Na[*o*-FESAN] (1:100) sample. At the figure left and middle top (bottom) are shown the lateral force forward (backwards) images corresponding to the topographies of Figure 7 - images a and c in the manuscript. Right panels from top to bottom are the topography profile and corresponding friction (green) data extracted from the separated lateral force profiles depicted in the bottom panel. All line profiles were taken at the same surface location for direct correlation between morphological details and chemical nature of the different surface regions. The Na[*o*-FESAN] fibers have a friction 75% lower than the surrounding DNA aggregates. The irregular rim on the round perimeter of the structures has the same frictional contrast as the small aggregates extended over the surrounding areas.

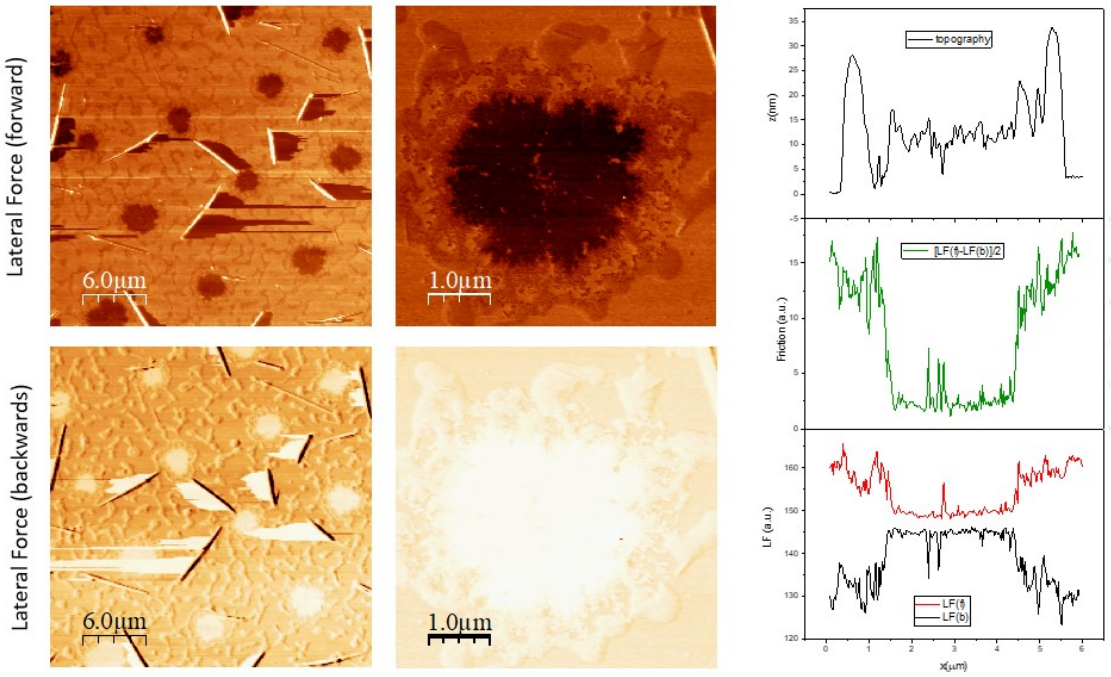

Figure S8. a) ESI-MS spectra of the CT-*ds*DNA/Na[*o*-FESAN] nanohybrid at the **positive mode**. b) ESI-MS spectra of the CT-*ds*DNA/Na[*o*-FESAN] nanohybrid at the **negative mode**; peak displays isotopic (-1) distribution. c) Magnification of the positive mode in the range 400-650 m/z; the peaks display isotopic (+1) distribution.

a)

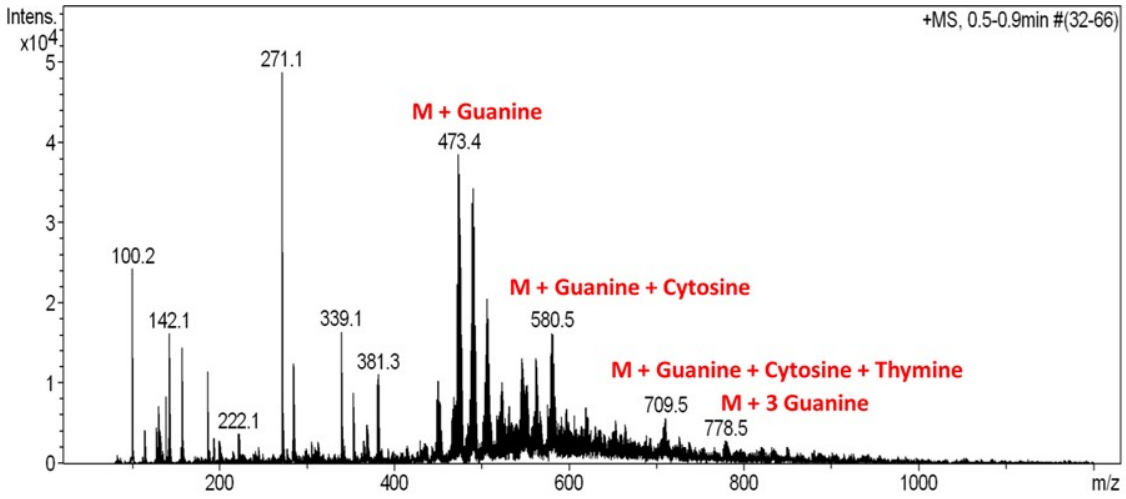

b)

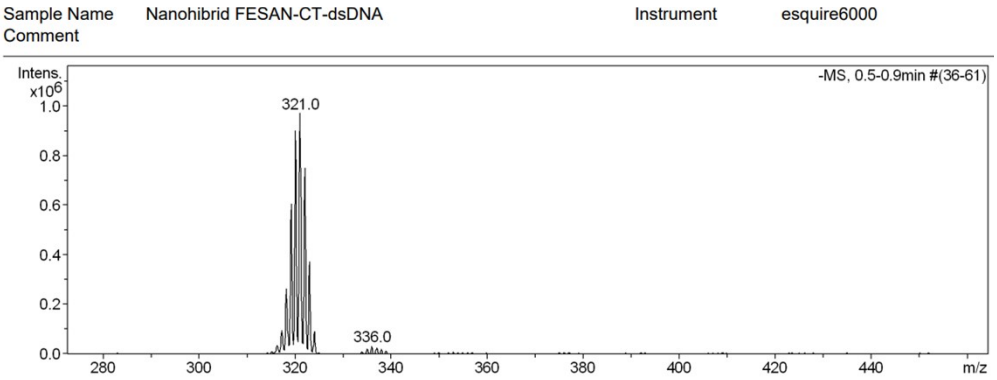

c)

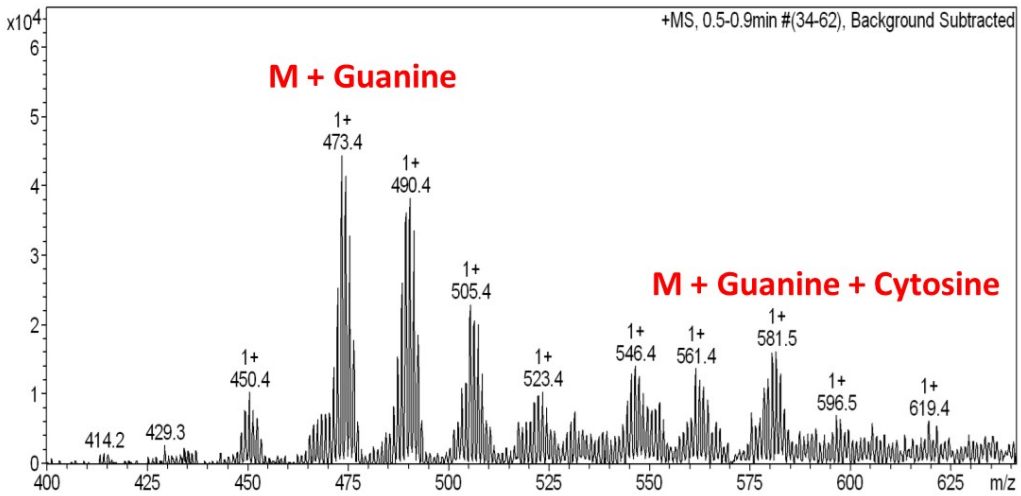

Figure S9. a) MALDI-TOF-MS run in the range 199.0 – 5013.0 m/z at the **negative mode** in the **absence of matrix**: CT-*ds*DNA (at the top), the hybrid CT-*ds*DNA/Na[*o*-FESAN] diluted 100 times in H_2O (at the middle) and the hybrid CT-*ds*DNA/Na[*o*-FESAN] diluted 100 times in acetone (at the bottom). b) Spectrum of the CT-*ds*DNA (reference) with the corresponding peaks number that are the ones used in Table S2 for the assignation of the nanohybrids peaks.

a)

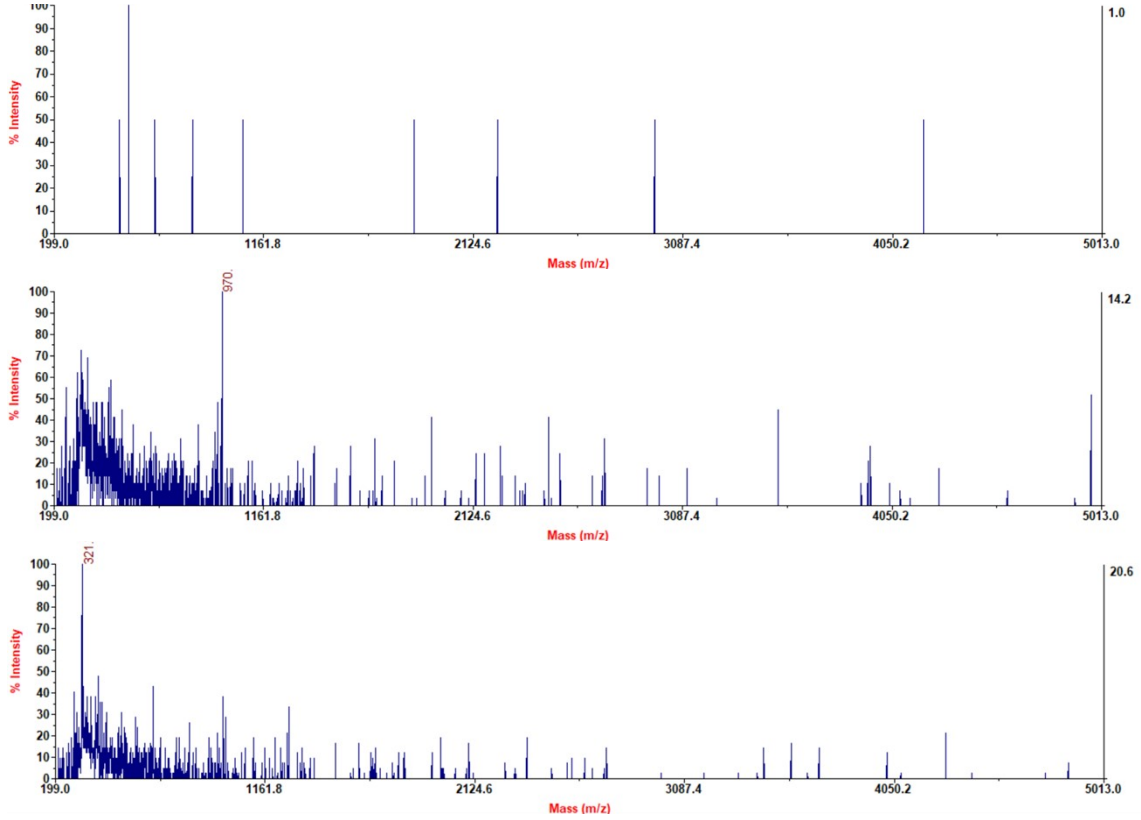

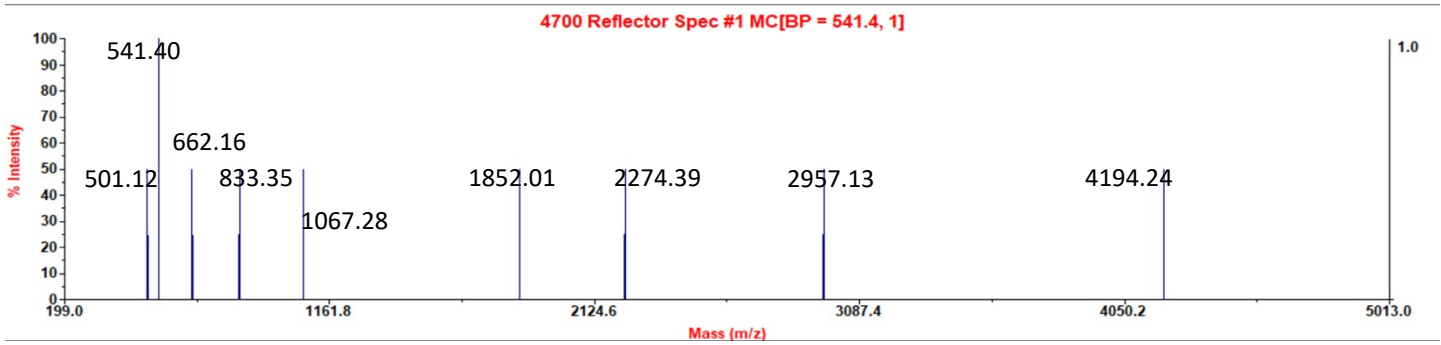

b)

Figure S10. Magnification of the MALDI-TOF-MS spectra at the **negative mode** of CT-*ds*DNA (blue) and CT-*ds*DNA/Na[*o*-FESAN] (red) samples diluted 100 times in water (Figure S9a top and middle) in the different zones: a) from 200 m/z to 1400 m/z; b) from 1400 m/z to 2600 m/z and c) 2600 m/z to 5000 m/z.

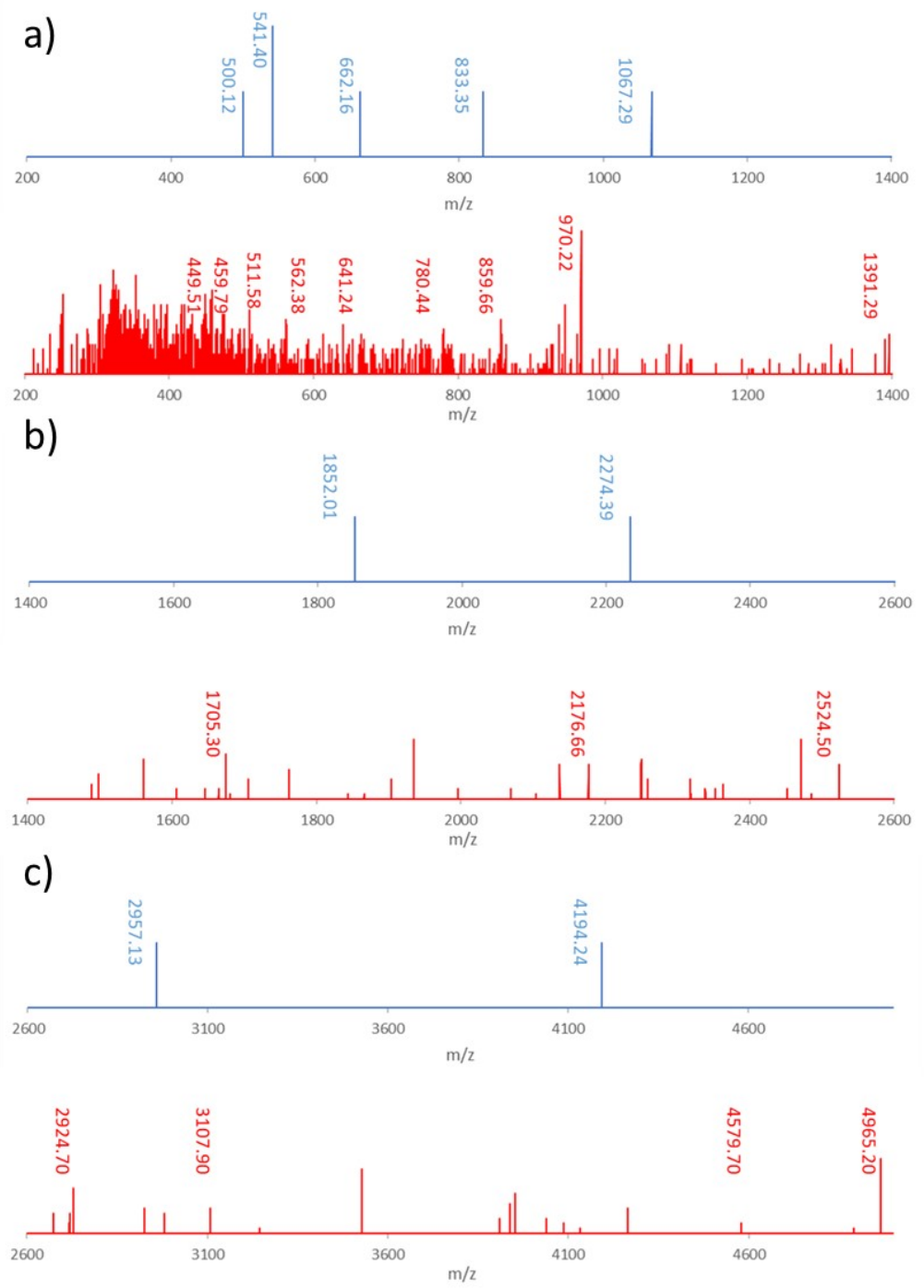

Figure S11. MALDI-TOF-MS spectra of the CT-*ds*DNA/Na[*o*-FESAN] nanohybrid diluted 100 times **in water** (up in red) and CT-*ds*DNA/Na[*o*-FESAN] nanohybrid diluted 100 time **in acetone** (down in marooned): d) from 200 m/z to 1400 m/z, e) from 1400 m/z to 2600 m/z and f) 2600 m/z to 5000 m/z.

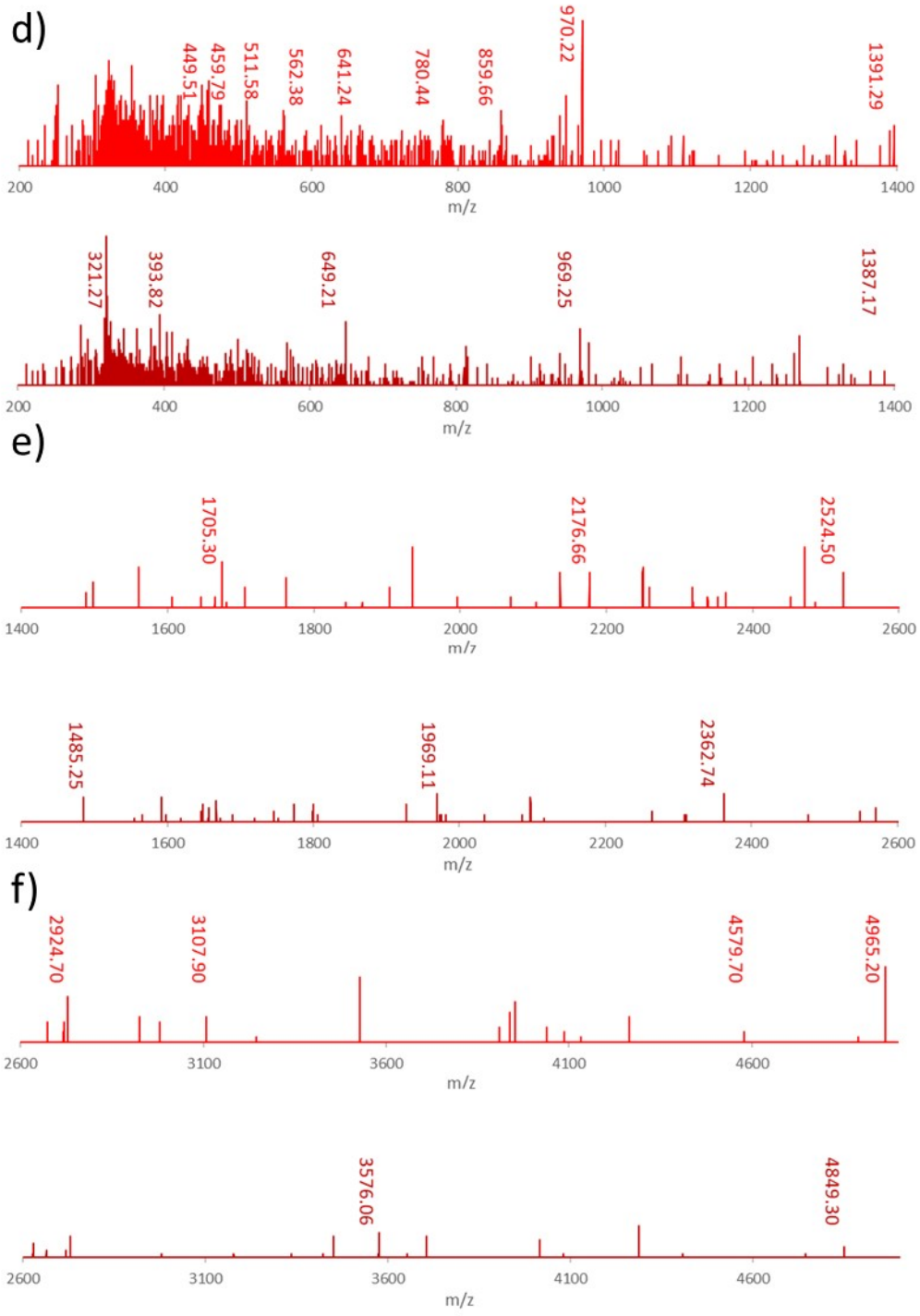

Figure S12. MALDI-TOF-MS at the **negative mode** of CT-*ds*DNA (the reference). Range: 0-3500 Da; DHB (**matrix**); 70 (attenuation 30%); laser 7000 shots. Magnification at high molecular peaks.

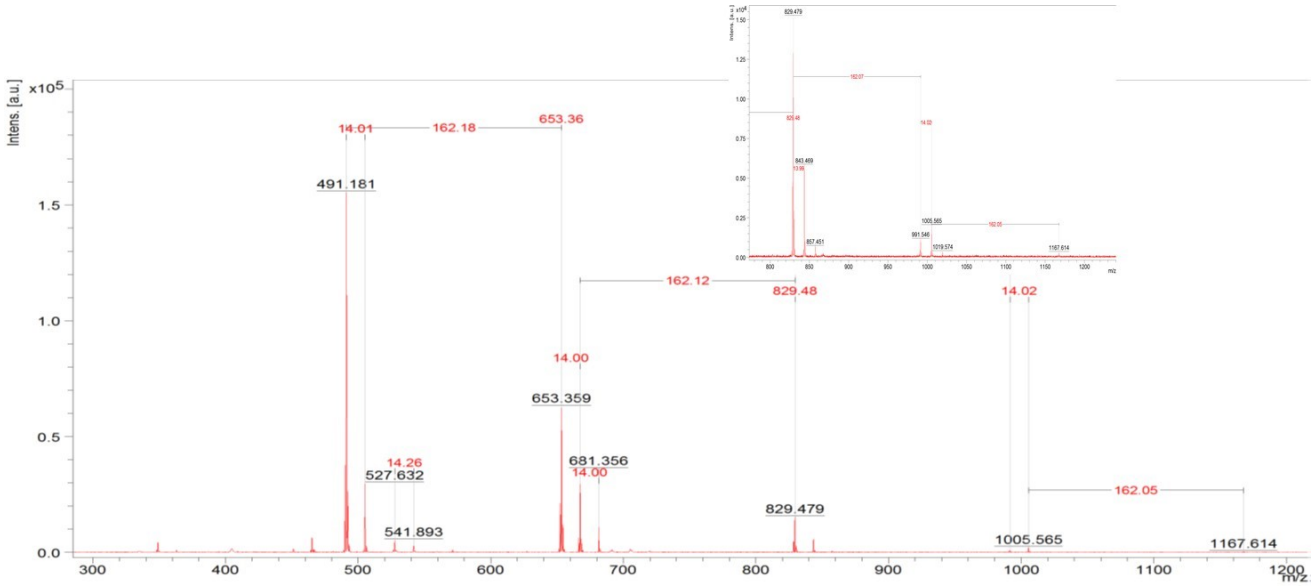

Figure S13. a) MALDI-TOF-MS spectrum at the **negative mode** of the CT-*ds*DNA/Na[*o*-FESAN] nanohybrid diluted 100 times **in water**. Range: 0-3500 Da; **DHB** (matrix); 70 (attenuation 30%); laser 7000 shots. b) Magnification and theoretical mass spectra of the peaks at 437.28, 473.44 and, 647.61 m/z; (z=1).

a)

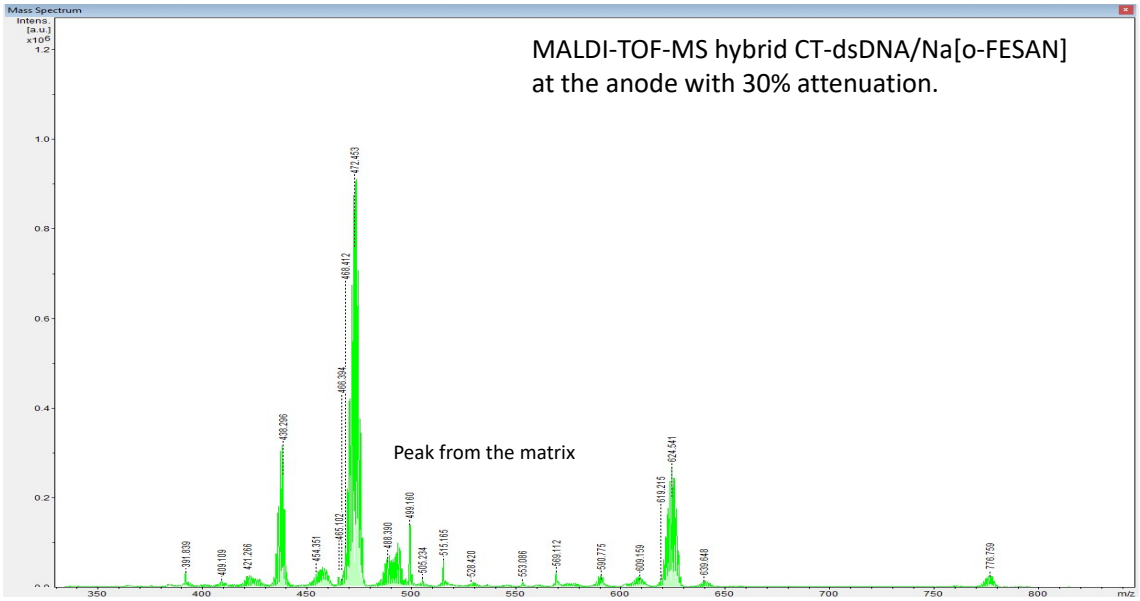

b)

M = Molecular weight of the anion [*o*-FESAN] = 320.660

- Anode: **437.284(M+116.63 (citosine))**; **473.440(M+152.78 (guanine))**; 624.611(**M+304.05 (two guanines)+H⁺**

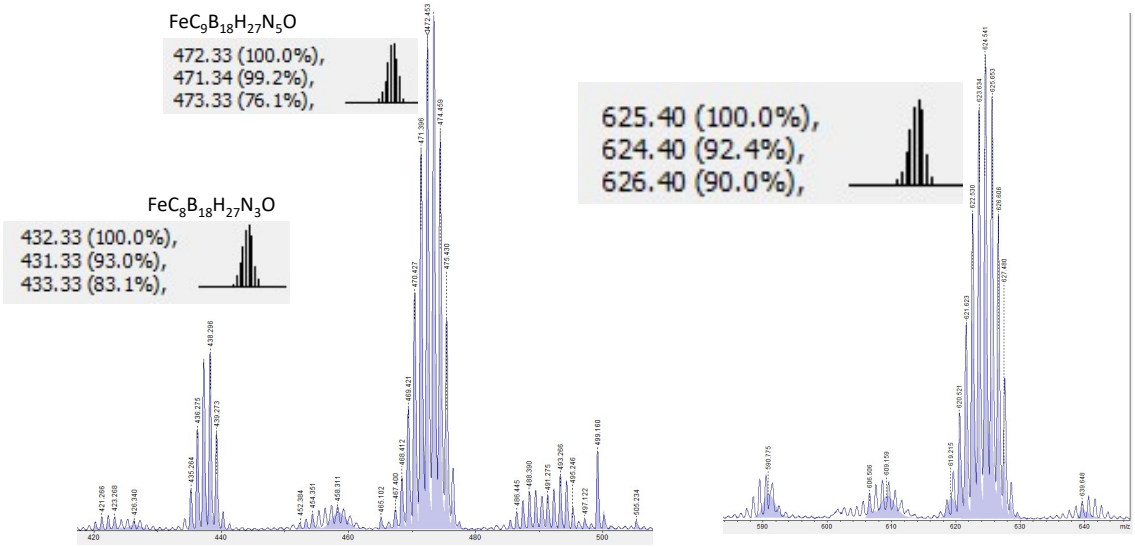

Table S1. Elemental analysis of the dry nanohybrid CT-*ds*DNA/Na[o-FESAN] and the dry CT-*ds*DNA.

	%C		%H	%N	C:H:N
Reference: dry CT-*ds*DNA					
	28.94		3.72	12.69	
	28.93		3.87	12.77	
Average	28.94		3.80	12.73	**2.65:4.18:1**
rsd (%)	0.01		2.84	0.45	
Dry CT-*ds*DNA/Na[*o*-FESAN]					
	22.64		6.07	4.45	
	22.55		6.53	4.08	
Average	22.60		6.30	4.27	**6.71:22.50:1**
rsd (%)	0.28		5.12	6.13	

Limit of quantification C, H, N = 0.1%

Reference: (dry CT *ds*-DNA)
C 28.94/12 = 2.41
H 3.80
N 12.73/14 = 0.91 **C:H:N = 2.65:4.18:1**

Sample: dry [*o*-FESAN]$^-$/CT *ds*-DNA
C 22.60/12 = 1.88
H 6.30
N 4.27/14 = 0.28 **C:H:N = 6.71:22.5:1**

Results related to C:

6.71 – 2.65 = 4.06 Per each atom of N in the reference (CT *ds*-DNA) there are 4 extra C atoms that corresponds to one molecule of [*o*-FESAN]$^-$, which empirical molecular formula is $FeC_4B_{18}H_{22}$).

Results related to H:

22.50 – 4.18 = 18.32 Per each atom of N in the reference (CT *ds*-DNA) there are 18 extra H atoms that approx. corresponds to one molecule of [*o*-FESAN]$^-$, which empirical molecular formula is $FeC_4B_{18}H_{22}$).

From the elemental analysis:

1) There are 12.73g of N per each 100g of **dry CT-*ds*DNA**.

2) There are 4.27g of N per each 100g of **dry [o-FESAN]-/CT ds-DNA nanohybrid.**

The amount of **dry CT-*ds*DNA** in the 100 g of **dry [o-FESAN]-/CT ds-DNA nanohybrid** is **33.54g**

100g **dry CT-*ds*DNA** 12.73g N

x 4.27g N

x= 33.54g of **dry CT-*ds*DNA** in 100g of **dry [o-FESAN]-/CT ds-DNA nanohybrid**

100g of **dry [o-FESAN]-/CT ds-DNA nanohybrid** contain 33.54g of **dry CT-*ds*DNA** and 66.46g of [*o*-FESAN]$^-$.

Number of mols of **CT-*ds*DNA** = 33.54 / 662 = **0.051**

Number of mols of **[*o*-FESAN]**$^-$= 66.46 / 320.66 = **0.207**

Ratio **[*o*-FESAN]**$^-$ **/ CT-*ds*DNA** = **4**

Molecular weight of a pair base of **CT-*ds*DNA** = 662

Molecular Weight of [*o*-FESAN]$^-$ = 320.66

Table S2. The anodic peaks of the MALDI-TOF-MS spectra of the CT-*ds*DNA (as the reference) and the nanohybrid CT-*ds*DNA/Na[*o*-FESAN] when the spectra were run **in the absence of any matrix** (see Figure S. To emphasize: i) all peaks correspond to z=1 and ii) the m/z of the anion [*o*-FESAN]$^-$ does not appear in the nanohybrid CT-*ds*DNA/Na[*o*-FESAN] spectrum, which fully supports that all the anionic [*o*-FESAN]$^-$ cluster molecules are bonded to the CT-*ds*DNA biopolymer.

m/z signals	**m/z**
CT-*ds*DNA	**Nanohybrid CT-*ds*DNA/Na[*o*-FESAN]**
	449.51 = 1 [*o*-FESAN]$^-$ + 1 Thymine
	459.79 = 1 [*o*-FESAN]$^-$ + 1 Adenine
501.12	511.58
541.40	562.38
662.16	641.24 = **2 [*o*-FESAN]$^-$**
	780.44 = 320.66 (**1 [*o*-FESAN]$^-$**) + **459.78 (1 [*o*-FESAN]$^-$ + 1 Adenine)** = **2 [*o*-FESAN]$^-$ + 1 Adenine**
833.35	859.66 = **539.00** + 320.66 (**1 [*o*-FESAN]$^-$**)
	970.22 = **667.56** + 2x151.11 (**1 Guanine**)
1067.28	1391.29 = **833.35** + 320.66 (**1 [*o*-FESAN]$^-$**) + 126.11 (**1 Thymine**)+ 111.1 (**1 Cytosine**)
	1705.3 = **1064.0** + 641.32 (**2 [*o*-FESAN]$^-$**)
1852.01	2176.66 = **1856.**00 + 320.66 (**1 [*o*-FESAN]$^-$**)
2274.39	2524.5 = **2274.39** + 2x 151.13 (**2 Guanines**)
	2924.7 = **2274.39** + 3x 151.13 (**3 Guanines**) + 2x126.11 (**2 Thymine**)
2957.13	3107.9 = **2957.13** + 150.77 (**1 Guanine**)
4194.24	4579.7 = **4194.24** + 150.77 (**1 Guanine**) + 111.11 (**1 Cytosine**) + 126.11 (**1 Thymine**)
501.12	4965.2 = **4194.24** + 150.77 (**2 Guanine**) + 111.11 (**2 Cytosine**) + 126.11 (**2 Thymine**)

Table S3. Analysis of the XPS spectra of deconvoluted B 1s, P 2p and N 1s for the CT-*ds*DNA/Na[*o*-FESAN] nanohybrid, Na[*o*-FESAN]$^-$ and *ds*DNA. The indicated core level binding energy (BE) for each element and material sample has been determined using as in-situ reference the C 1s at 284.8eV (survey spectra in Figure S1 in the Supporting Information). New peaks, clearly appearing in the nan-hybrid material respect to the pure initial compounds, are indicated (∗). For simplicity, instead of total peak area, the Intensity given is the calculated peak height in counts per second (CPS) extracted from the experimental fits before (after) subtracting the adequate baseline or background intensity.

	B 1s		**P 2p**		**N 1s**	
	BE (eV)	Intensity (CPS)	BE (eV)	Intensity (CPS)	BE (eV)	Intensity (CPS)
DNA			131.5	2457.09(1536.75)	397.8	7499(2455.84)
			134.2	1608.4(688.06)	399.7	7522.23(2479.07)
Na[*o*-FESAN]	188.6	2956.5(2909.2)				
	189.5	718(670)				
Nanohybrid	185.9 *	451.51(230.45)	122.2 *	1123.32(277.52)	396.5	4945.12(225.12)
			131.5	1268.3(422.5)		
	188.7	1870.6(1649.57)	134.1	2690.2(1844.4)	399.9	6444.9(1724.9)
			138.05 *	1093.2(247.4)		

Figure S14. a) ^{11}B-NMR spectra of Na[*o*-FESAN] in D_2O with the chemical shift numbers of the Boron vertices B(6), B(5,11), B(9,12), B(10), B(4,7) and B(8) from down to high field.[1] b) ^{1}H-NMR spectra of Na[*o*-FESAN] in D_2O.[1] c) The CV wave of Na[*o*-FESAN]. $E_{1/2}$ = -1.00V versus F_c^+/F_c.[2] d) Solubility study of Na[3,3'-Fe(1,2-$C_2B_9H_{11}$)$_2$], Na[*o*-FESAN] in H_2O; Plot of absorbance *vs.* concentration.[2]

a)

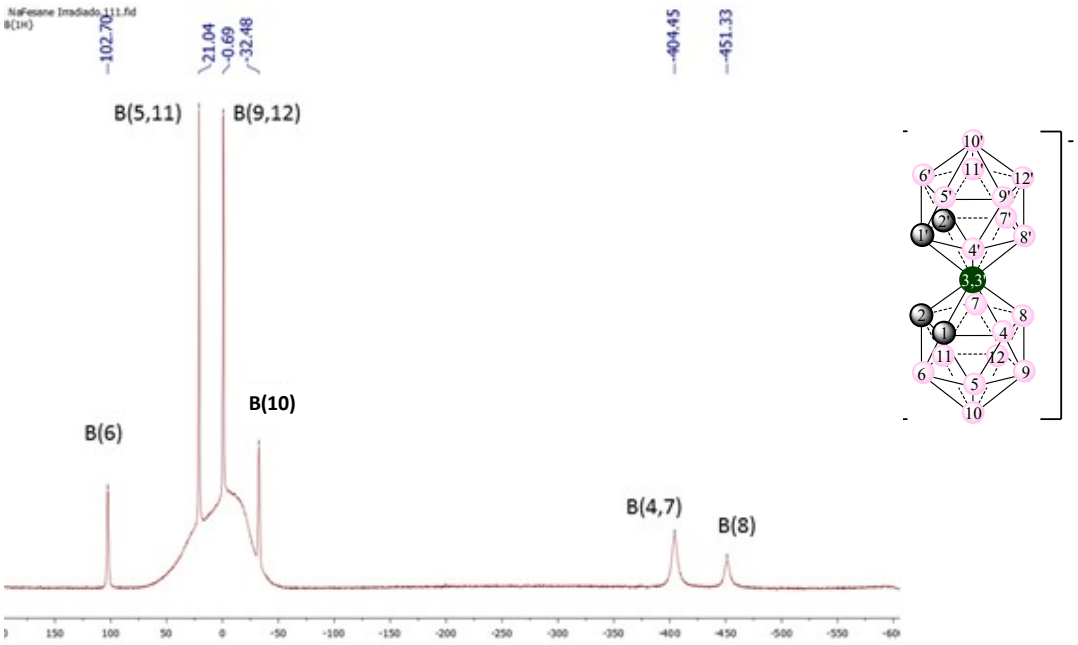

b)

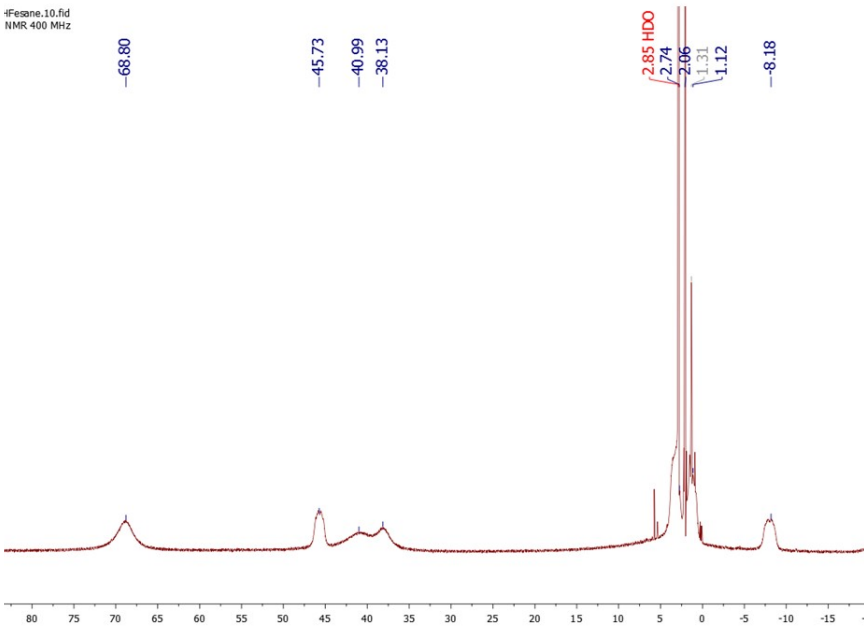

c)

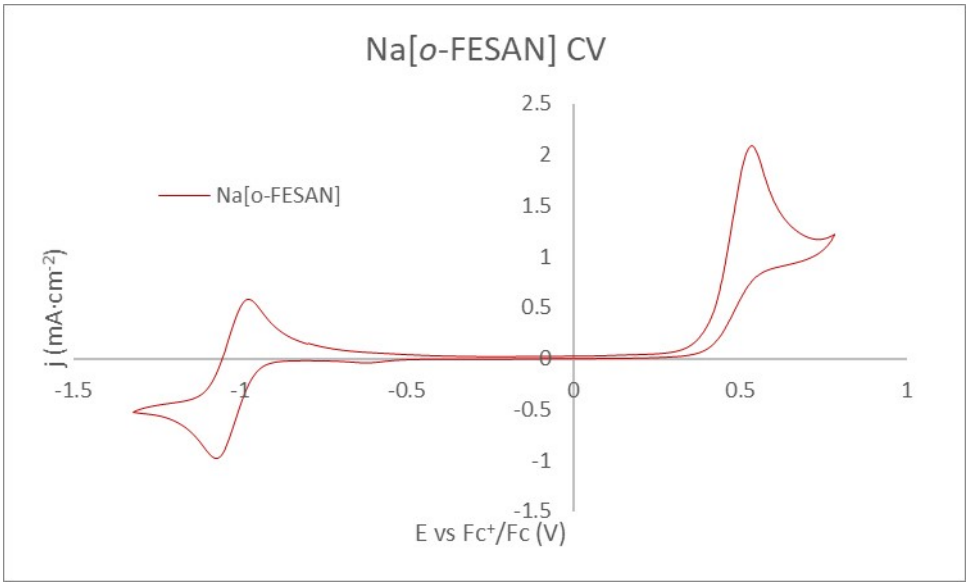

d) Solubility of Na[3,3'-Fe(1,2-$C_2B_9H_{11})_2$] in water 1.247±0.018 M or 484.72±7.01 g/L

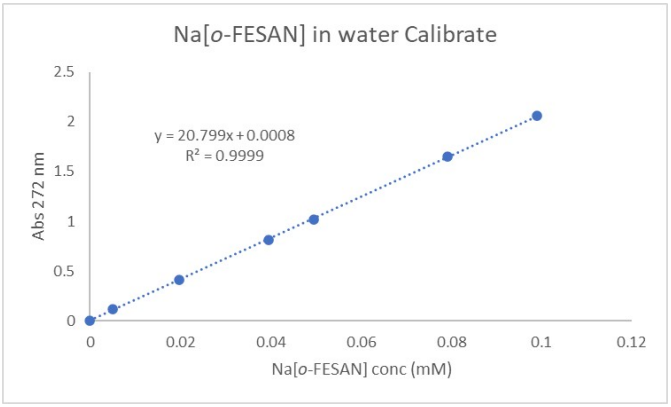

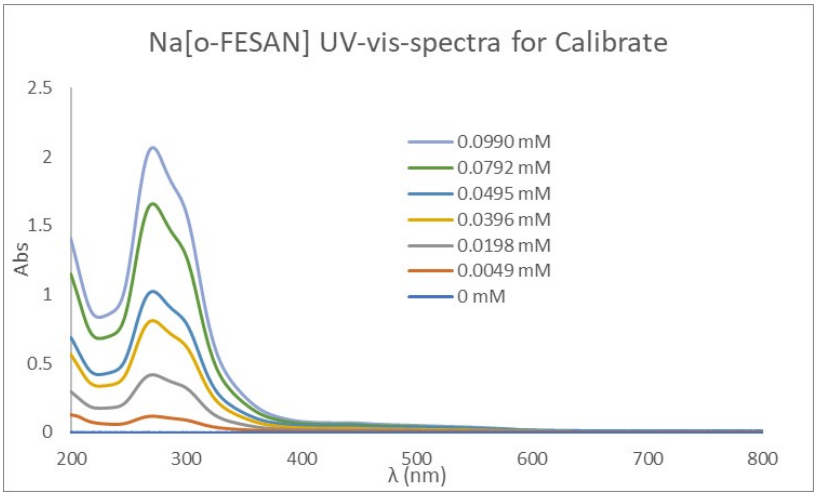

References

1 T. Garcia-Mendiola, V. Bayon-Pizarro, A. Zaulet, I. Fuentes, F. Pariente, F. Teixidor, C. Viñas and E. Lorenzo, Chem. Sci., 2016, 7, 5786–5797.

2 I. Bennour, M. N. Ramos, M. Nuez-Martínez, J. A. M. Xavier, A. B. Buades, R. Sillanpää, F. Teixidor, D. Choquesillo-Lazarte, I. Romero, M. Martinez-Medina and C. Viñas